



## Pharmaceutical nanotechnology

## High speed electrospinning for scaled-up production of amorphous solid dispersion of itraconazole



Zsombor K. Nagy<sup>a,\*</sup>, Attila Balogh<sup>a</sup>, Balázs Démuth<sup>a</sup>, Hajnalka Pataki<sup>a</sup>, Tamás Vigh<sup>a</sup>, Bence Szabó<sup>a,b</sup>, Kolos Molnár<sup>b</sup>, Bence T. Schmidt<sup>a,c</sup>, Péter Horák<sup>c</sup>, György Marosi<sup>a</sup>, Geert Verreck<sup>d</sup>, Ivo Van Assche<sup>d</sup>, Marcus E. Brewster<sup>d</sup>

<sup>a</sup> Budapest University of Technology and Economics, Department of Organic Chemistry and Technology, Hungary

<sup>b</sup> Budapest University of Technology and Economics, Department of Polymer Engineering, Hungary

<sup>c</sup> Budapest University of Technology and Economics, Department of Machine and Industrial Product Design, Hungary

<sup>d</sup> Janssen Research and Development, Belgium

## ARTICLE INFO

## Article history:

Received 8 December 2014

Received in revised form 12 January 2015

Accepted 13 January 2015

Available online 14 January 2015

## Keywords:

Electrospinning

Itraconazole

Amorphous solid dispersion

Scaling-up

Dissolution enhancement

Continuous nanoformulation

## ABSTRACT

High speed electrospinning (HSES), compatible with pharmaceutical industry, was used to demonstrate the viability of the preparation of drug-loaded polymer nanofibers with radically higher productivity than the known single-needle electrospinning (SNES) setup. Poorly water-soluble itraconazole (ITRA) was formulated with PVPVA64 matrix polymer using four different solvent-based methods such as HSES, SNES, spray drying (SD) and film casting (FC). The formulations were assessed in terms of improvement in the dissolution rate of ITRA (using a “tapped basket” dissolution configuration) and analysed by SEM, DSC and XRPD. Despite the significantly increased productivity of HSES, the obtained morphology was very similar to the SNES nanofibrous material. ITRA transformed into an amorphous form, according to the DSC and XRPD results, in most cases except the FC samples. The limited dissolution of crystalline ITRA could be highly improved: fast dissolution occurred (>90% within 10 min) in the cases of both (the scaled-up and the single-needle) types of electrospun fibers, while the improvement in the dissolution rate of the spray-dried microspheres was significantly lower. Production of amorphous solid dispersions (ASDs) with the HSES system proved to be flexibly scalable and easy to integrate into a continuous pharmaceutical manufacturing line, which opens new routes for the development of industrially relevant nanopharmaceuticals.

© 2015 Elsevier B.V. All rights reserved.

## 1. Introduction

One of the largest challenges in the field of pharmaceutical technology is the enhancement of drug release from orally taken solid dosage forms. Most of the recently developed active pharmaceutical ingredients (APIs) and candidates in the contemporary drug pipelines are poorly soluble in the aqueous gastrointestinal fluids. It is a consequence of the practice of the high-throughput screening method, hit-to-lead optimization and the nature of the chemical space of therapeutic targets (Keserű and Makara, 2009; Lipinski et al., 1997; Lipinski, 2000; Prentis et al., 1988). Most of such drugs are classified as class II (low solubility

but high permeability) according to the Biopharmaceutical Classification System (BCS) (Amidon et al., 1995). Thus, the main absorption-limiting factor of BCS II drugs is generally drug dissolution (both the rate and the extent) (Pouton, 2006). Drug formulation can play a determining role in the enhancement of the dissolution and hence of the bioavailability of these drugs.

In the age of nanotechnology, new techniques became available to improve dissolution. One of the most promising nanotechnology-based approaches is electrostatic spinning, which is a remarkably simple and continuous way for producing nanofibers (Lukas et al., 2009). Such nanofibers proved to be valuable in the fields of filtration (Li et al., 2013a), composites (Molnár et al., 2014), textiles, catalysts (Sóti et al., 2014), medicine anti-counterfeiting (Huang et al., 2010) and medical researches (wound dressing (Rosic et al., 2013), wound healing (Macri et al., 2012; Pelipenko et al., 2013), topical therapy (Huang et al., 2012a,b, 2014; Nagy et al., 2014) and tissue engineering (Kostakova et al., 2014; Driscoll et al., 2013; Nagy et al., 2013)). Electrospinning technology has recently

\* Corresponding author at: Budapest University of Technology and Economics, Organic Chemistry and Technology, Muegyetem rkp. 3, 1111 Budapest, Hungary. Tel.: +36 1463 1424; fax: +36 1463 3648.

E-mail address: [zsknagy@oct.bme.hu](mailto:zsknagy@oct.bme.hu) (Z.K. Nagy).

attracted an increased academic and industrial attention because it is an effective way to prepare nanofibrous drug formulations with an enhanced dissolution (Verreck et al., 2003; Brewster et al., 2004; Nagy et al., 2010,c; Yu et al., 2013a,b,c,c; Vrbata et al., 2013; Wagner et al., 2011; Balogh et al., 2014; Li et al., 2013b; Williams et al., 2012; Yan et al., 2014) by combining a number of strategies and approaches. These include increasing the specific surface area; forming nano-amorphous solid dispersion (NASD); enhancing wettability and solubility; achieving supersaturation and hindering precipitation (Nagy et al., 2012). Owing to these remarkable advantages, the number of publications about electrospun oral drug delivery systems is increasing dynamically. However, most of the researchers use the single-needle electrospinning (SNES) method without any scale-up attempts, which would be necessary for the industrial application of the technology in pharmaceutical manufacturing (Williams et al., 2012; Bohr et al., 2014; Hu et al., 2014).

Probably, one of the main obstacles to spreading and commercialization of drug delivery systems based on electrospun materials is the lack of an adequate pharma-industry-compatible scale-up of the technology, as it was pointed out by Hu et al. (2014) recently. Scale-up of electrospinning appears to be challenging for the pharmaceutical industry mainly because of the use of volatile solvents (e.g., ethanol, dichloromethane, methanol etc.), which seems to be incompatible with the scalable needleless electrospinning techniques published up to now (Niu and Lin, 2012; Kostakova et al., 2009). The presence of relatively large free liquid surface in these machines, where excessive solvent evaporation can take place, is hardly acceptable for industrial technologists for safety and technological reasons.

Consequently, development of a high-throughput electrospinning method, which is compatible with the pharmaceutical industry and capable for production on both laboratory and large scales (from ~100 mg to several kg), is needed. Exploitation of the exceptional inherent advantages of electrospinning regarding drug formulation is industrially feasible only in this way.

In order to step forward to the realization of a scalable pharma-electrospinning-based manufacturing, we developed a technology utilizing a rotating spinneret (Molnár et al., 2012), which can increase the productivity significantly. The throughput of this process was supposed to be increasable by increasing the rotational speed of the spinneret. Thus, the present work, regarding high speed electrospinning (HSES), aimed at maximizing productivity. This paper discusses the applicability of the HSES method for the preparation of amorphous solid dispersions using a model system consisting of PVPVA64 matrix and itraconazole (a widely investigated poorly water-soluble antifungal drug) in comparison with SNES and the conventional industrial technologies of film casting and spray drying. The performances of these methods and the characteristics of each product are compared in order to assess the similarities, differences, advantages and disadvantages of these technologies.

## 2. Materials and methods

### 2.1. Materials

Itraconazole (ITRA) was provided by Janssen Pharmaceutica (Beerse, Belgium). Kollidon<sup>®</sup> VA 64 (Copovidone, PVPVA64), provided by BASF as a kind gift, is a vinylpyrrolidone/vinylacetate amorphous copolymer (6:4) with a molecular weight in the range of 45–70 kDa.

### 2.2. Single-needle electrospinning

The electrostatic spinner used in the experiments was equipped with an NT-35 high voltage DC supply (Unitronik Ltd., Nagykanizsa, Hungary). The electrical potential applied on the spinneret electrode was 30 kV. A grounded aluminum plate covered with aluminum foil was used as a collector. The distance of the spinneret and the collector was 15 cm, and the experiments were performed at ambient temperature (25 °C). The polymer solution (Table 1) was dosed by means of an SEP-10S Plus type syringe pump (Aitecs, Vilnius, Lithuania). The dosing rate was 20 mL/h.

### 2.3. Scaled-up high speed electrospinning

The scaled-up electrospinning experiments were performed using a high speed electrostatic spinning setup consisting of a stainless steel spinneret with sharp edges and spherical cap geometry connected to a high speed motor. The polymer solution (Table 1) was fed with a SEP-10S Plus syringe pump with a flow rate of 1500 mL/h. The rotational speed of the spinneret was fixed at 40,000 rpm, and the voltage applied on it was 50 kV during the experiments (NT-65 high voltage DC supply Unitronik Ltd., Nagykanizsa, Hungary). The grounded collector covered with aluminum foil was placed 35 cm from the spinneret in all cases. The experiments were performed at ambient temperature (25 °C). The processed solutions were the same in the case of ES, HSES and FC for an easier comparison.

### 2.4. Spray drying

Spray drying was performed with a ProCepT 4M8-TriX spray dryer (Belgium) using a 0.4 mm two-fluid nozzle. The process parameters were as follows: atomization air pressure 0.4 bar, drying air temperature 70 °C, drying air flow 0.3 m<sup>3</sup>/min and feeding rate 150 mL/h.

### 2.5. Film casting

The solution of the polymer and the drug (Table 1) was cast into square-shaped silicon molds (3 × 50 × 50 mm) and subsequently dried in a drying oven (Smith and Klein H110W, Germany) at 40 °C for 24 h. The thickness of the prepared film was (150 ± 10) μm,

**Table 1**  
Comparison of the details of manufacturing using different solvent based methods.

Sample	Preparation method	Applied solvent	Dissolved PVPVA64 and ITRA (6:4) in 10 mL of solvent (g)	Flow rate (mL/h)	Productivity for dried material (g/h)
PVPVA64 + 40% ITRA SNES	Single needle electrospinning	CH <sub>2</sub> Cl <sub>2</sub> + EtOH (2:1)	3.75	20	6
PVPVA64 + 40% ITRA HSES	High speed electrospinning	CH <sub>2</sub> Cl <sub>2</sub> + EtOH (2:1)	3.75	1500	450
PVPVA64 + 40% ITRA SD	Spray drying	CH <sub>2</sub> Cl <sub>2</sub> + EtOH (2:1)	0.5	150	7.5
PVPVA64 + 40% ITRA FC	Film casting	CH <sub>2</sub> Cl <sub>2</sub> + EtOH (2:1)	3.75	–	–

measured with a pro-max electronic digital caliper (NSK, Tokyo, Japan). For dissolution tests the fragile film was chopped into small shreds (i.e., no grinding was performed).

### 2.6. Differential scanning calorimetry

Differential scanning calorimetry (DSC) measurements were carried out using a TA Instruments Q2000 DSC apparatus (New Castle, Delaware) (sample weight: ~2–3 mg, closed aluminum pan, 50 mL/min nitrogen purge gas flow). The temperature program consisted of an initial isothermal period that lasted for 1 min at 25 °C, with subsequent linear heating from –25 °C to 200 °C at a rate of 10 °C/min. Purified indium standard was used to calibrate the instrument.

### 2.7. Scanning electron microscopy (SEM)

Morphology of samples was investigated by means of a JEOL 6380LVa (JEOL, Tokyo, Japan) type scanning electron microscope. Each specimen was fixed with conductive double-sided carbon adhesive tape and sputter-coated with gold–palladium alloy prior to examination. Applied accelerating voltage and working distance were 15–25 kV and 12–16 mm, respectively.

### 2.8. X-ray diffraction (XRD)

Powder X-ray diffraction patterns were recorded with a PANalytical X'pert Pro MDP X-ray diffractometer (Almelo, The Netherlands) using Cu-K $\alpha$  radiation (1.542 Å) and Ni filter. The applied voltage was 40 kV, while the current was 30 mA. The untreated materials, physical mixture (mixed in a mortar with a pestle) and the fibrous samples were analyzed between  $2\theta$  angles of 4° and 42°.

### 2.9. In vitro dissolution measurement

Dissolution studies were performed using a modified Pharmatest PTWS 600 dissolution tester (Pharma Test Apparatebau AG, Hainburg, Germany). The modification was undertaken so that the instrument could be operated with an apparatus called tapped basket, which is a combination of the USP I (basket) and the USP II (paddle) apparatuses. The modification could be implemented and can be described very simply. A helical path fixed on the axis of the paddle gradually lifts the basket during one rotation of the paddle, then lets it fall to the starting point of the cycle in an instant. The basket closed on the top never emerges from the dissolution liquid during the dissolution period (Fig. 3). Samples equivalent to 50 mg of ITRA were weighted without any pretreatment into the dissolution baskets and immersed in 900 mL of 0.1 M HCl dissolution medium kept at a constant temperature of (37 ± 0.5) °C while the paddle frequency was always kept at 50 rpm. An on-line coupled Agilent 8453 UV–vis spectrophotometer (Hewlett-Packard, Palo Alto, USA) was used to measure the concentration of dissolved ITRA at a wavelength of 254 nm. The percentage of dissolution could be readily calculated based on the calibration curve of ITRA in 0.1 M HCl.

## 3. Results and discussion

Overviewing the relevant scientific literature revealed that no results have been published up to now regarding the scale-up of the production of nanofibrous pharmaceuticals. Accordingly, the present research work focused on the evaluation of HSES technology as a promising candidate to meet the requirements of pharmaceutical industry (e.g., high throughput, volatile solvent compatibility), in comparison with reference methods

(considering e.g., product quality, productivity, solvent consumption, manufacturing temperature etc.).

The model system selected for this investigation contained PVPVA64 as matrix forming polymer and ITRA as poorly water-soluble drug. Our intention was to prepare amorphous solid dispersions from the polymer and the API (active pharmaceutical ingredient) by using HSES, SNES, SD and FC techniques in order to enhance the dissolution of ITRA.

### 3.1. Comparison of technological aspects (SNES, HSES, SD)

The production rate of SNES is limited to ~0.1–2 g of dry product per hour (Lukas et al., 2009), which cannot fulfill the quantity demand of pharmaceutical manufacturing. Recently published papers dealing with electrospun oral drug delivery systems reported similar productivities (Nagy et al., 2010, 2014; Verreck et al., 2003; Brewster et al., 2004,b; Yu et al., 2013a,b; Vrbata et al., 2013; Wagner et al., 2011; Balogh et al., 2014; Li et al., 2013b; Williams et al., 2012; Ignatious et al., 2010). High speed electrospinning (HSES) combines electrostatic (Lukas et al., 2008) and high speed rotational (Sebe et al., 2013) jet generation and fiber elongation, thus improving the productivity significantly (Table 1).

In our experiments (described in Section 2) a feeding rate and a productivity 75 times higher than those of SNES could be achieved with HSES, which meant a feeding rate of 1500 mL/h and ~450 g of solid product in an hour in the case of HSES. The lab-scale spray dryer showed a much lower productivity (7.5 g/h) with a significantly higher specific solvent consumption (~20 mL/1 g dry product) was used to achieve the required small particle size, 2–20  $\mu$ m compared to the HSES method (2.7 mL/g). A heated air stream in a longer and wider drying column would be needed to spray-dry particles with a productivity of ~0.5 kg/h, the capacity of HSES. The drying time of the sprayed particles is generally significantly longer than in the case of ES (which is <1 s) because in the latter case submicronic objects with considerably higher specific surface area available for solvent evaporation are produced. Moreover, electrostatic charging significantly facilitates solvent evaporation (Lukas et al., 2009).

The productivity result of ~450 g/h achieved using HSES means that a production rate of ~10.8 kg/day is possible with this technology. By multiplying the high speed spinnerets, the total output can be further increased. This scaled-up, continuous and flexible manufacturing process seems to be capable of fulfilling the capacity requirements of pharmaceutical industry.

### 3.2. Morphology

A critical issue when electrospinning is attempted to be realized on a larger scale using HSES is the morphology of the product. As the combination of high speed rotation and electrostatic forces intensifies jet generation and fiber elongation, the question arises whether the fibrous structure changes consequently. The results confirmed that despite the differences between SNES and HSES in fiber formation mechanism and output, the obtained morphologies can be quite similar as shown in Fig. 1.

The produced solid dispersions were both fibrous with diameters in the range of 0.5–2  $\mu$ m. Among this major proportion of fibers, some micrometer-sized beads were observable as well. In the case of the HSES sample, the occurrence of beads was relatively higher comparing to the SNES fibers. Further investigations must be done for a better understanding of the mechanism of bead formation during high speed electrospinning (which is an ongoing work).

The morphology of the spray-dried powder was also investigated. The powder contained regular spheres with diameters

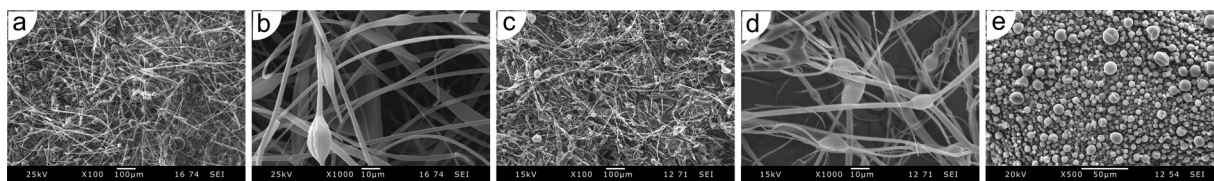


**Fig. 1.** Scanning electron microscopic images of PVPVA64+40% ITRA solid dispersions prepared by (a and b) single-needle electrospinning, (c and d) high speed electrospinning and (e) spray drying.

between 2 and 20  $\mu\text{m}$ . No crystalline phases were observable in the cases of electrospun fibers and spray dried spheres.

### 3.3. DSC and XRPD

In order to investigate the physical state of ITRA in the prepared solid dispersions, differential scanning calorimetry measurements were performed. The interpretation of the results is based on former studies describing the glassy state transitions of ITRA in solid dispersions (Six et al., 2001). According to the DSC thermograms shown in Fig. 2, the SNES, HSES, SD PVPVA64+40% ITRA samples were amorphous. The melting peak of ITRA at 166  $^{\circ}\text{C}$  does not appear in the curves; only a wide endotherm could be detected, which is related to the water loss of the PVPVA64 matrix.

In turn, the cast film containing 40% ITRA with the same polymeric matrix could not be prepared in a fully amorphous form despite the relatively fast evaporation of the applied volatile solvents. Well detectable melting peak of ITRA could be observed in the cast film indicating the phase separation of the drug and the polymer matrix.

According to the conventional way to investigate crystallinity in solid dispersions, X-ray powder diffraction (XRPD) was also performed, the result of which is shown in Fig. 2. The pure crystalline API served as reference. The lack of peaks suggests that

the API in the SNES, HSES and SD samples turned into an amorphous form during processing. In the case of the cast film, the XRPD analysis gave further evidence of the crystalline phase being present in the sample.

### 3.4. Dissolution results

In vitro studies were carried out to investigate the dissolution characteristics of the PVPVA64+40% ITRA samples. However, to obtain these results a new way of dissolution testing needed to be introduced (see Fig. 3). The rationale of the development of this novel dissolution method can be summarized with the following arguments. A drug with poor water solubility incorporated into a hydrophilic polymer carrier exerts a well-known hydrophobization effect on the solid dispersion. If either basket (USP type I) or paddle (USP type II) method is used, the tested sample gets stuck at the top of the basket or on the surface of the dissolution medium, in spite of the continuous rotating movement. The experiments performed these ways exhibited high variability and poor reproducibility, which could be attributed to the residual air between and around the particles. The key idea to resolve this issue was that the residual air content should be somehow removed. This could be managed using a periodical movement perpendicular to the plane of the rotating motion of the dissolution fluid. This movement was induced by the built apparatus called “tapped basket” (Fig. 3). Besides the significantly improved reproducibility of the dissolution measurements, this simple technique is more biorelevant since the described movement models the behavior of the gastrointestinal tract much better than the standard basket and paddle dissolution methods, with special regard to gastric conditions including the non-negligible mechanical forces (Vardakou et al., 2011).

The dissolution results in Fig. 3 show significant improvements compared to crystalline ITRA. The PVPVA64+40% ITRA HSES and SNES samples showed very fast drug dissolution: more than 90% of ITRA was released in both cases within the first 10 min. Dissolution

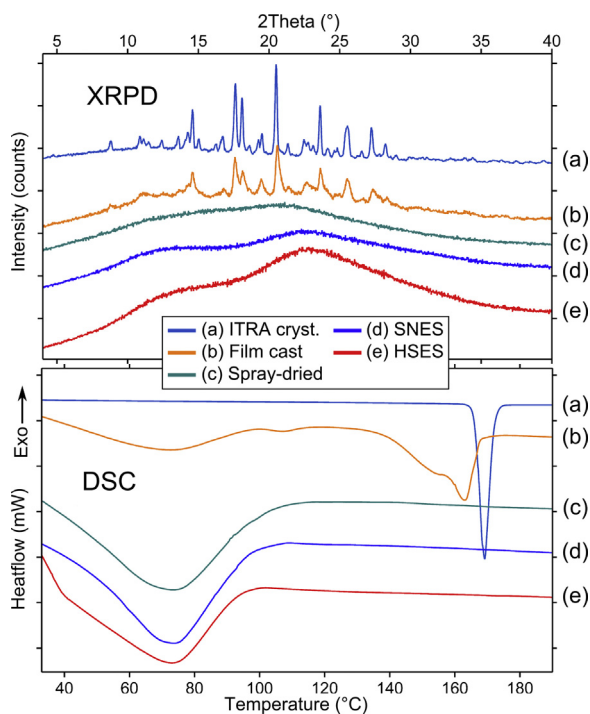


**Fig. 2.** X-ray powder diffraction patterns (XRPD) and differential scanning calorimetry thermograms (DSC) of (a) crystalline ITRA, and PVPVA64+40% ITRA solid dispersions prepared by (b) film casting, (c) spray drying, (d) single needle electrospinning and (e) high speed electrospinning.

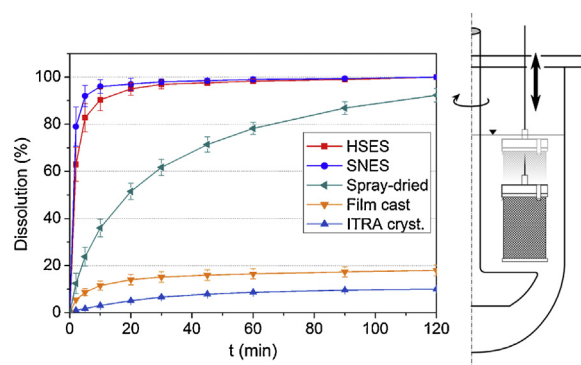


**Fig. 3.** Dissolution profiles of itraconazole [50 mg dose, 900 mL of 0.1 M HCl, tapped basket dissolution method (see the text and the illustration on the right), 50 rpm, 37  $^{\circ}\text{C}$ ]: PVPVA64-based high speed electrospun fibers (HSES), single needle electrospun fibers (SNES) and spray dried microspheres with 40% ITRA, and unprocessed crystalline ITRA. The error bars indicate  $\pm$  standard deviations ( $n=3$ ).

of spray-dried samples was almost total in 2 h but significantly slower than that of the electrospun samples, probably due to the smaller specific surface area of the spray-dried powder. The cast film exhibited only a slight improvement owing to the crystalline state of the API in the matrix.

#### 4. Conclusions

High speed electrospinning was used to demonstrate the viability of preparing drug loaded polymer nanofibers with radically higher productivity than with the single needle electrospinning setup. Poorly water-soluble ITRA was formulated with PVPVA64 matrix polymer using four different solvent-based methods: HSES, SNES, SD and FC. Despite the significantly increased productivity of HSES, the obtainable morphology was very similar to the SNES sample. ITRA transformed into an amorphous form, according to the DSC and XRPD results, in most cases except the FC samples due to considerably slower solvent evaporation from the cast material. The limited dissolution of crystalline ITRA could be highly improved: fast dissolution occurred (>90% within 10 min) in the cases of both (scaled-up and the single needle) types of electrospun fibers, while the improvement of the dissolution rate of the spray dried microspheres was significantly lower.

A 75-fold productivity improvement could be achieved by replacing the SNES process with HSES, with which a feeding rate of 1500 mL/h gives ~450 g solid product per hour. Thus, a ~10 kg/day production rate is possible with this technology. By multiplying the high speed spinnerets, the total output can be further increased. This scaled-up, continuous and flexible manufacturing process seems to be capable of fulfilling the technological and capacity requirements of pharmaceutical industry.

#### Acknowledgements

This work was financially supported by the New Széchenyi Development Plan (TÁMOP-4.2.1/B-09/1/KMR-2010-0002), by OTKA research fund (grant numbers K112644 and PD108975), by MedInProt Synergy Program and by the János Bolyai Research Scholarship of the Hungarian Academy of Sciences. The authors would like to express their gratitude to Éva Kiserdei for her excellent technical support.

#### References

- Amidon, G.L., Lennernäs, H., Shah, V.P., Crison, J.R., 1995. A theoretical basis for a biopharmaceutical drug classification: the correlation of in vitro drug product dissolution and in vivo bioavailability. *Pharm. Res.* 12, 413–420.
- Balogh, A., Drávavölgyi, G., Faragó, K., Farkas, A., Vigh, T., Sóti, P.L., Wagner, I., Madarász, J., Pataki, H., Marosi, G., Nagy, Z.K., 2014. Plasticized drug-loaded melt electrospun polymer mats: characterization, thermal degradation, and release kinetics. *J. Pharm. Sci.* 103, 1278–1287.
- Bohr, A., Boetker, J.P., Rades, T., Rantanen, J., Yang, M., 2014. Application of spray-drying and electrospinning/electrospinning for poorly water-soluble drugs: a particle engineering approach. *Curr. Pharm. Des.* 20, 325–348.
- Brewster, M.E., Verreck, G., Chun, I., Rosenblatt, J., Mensch, J., Van Dijck, A., Noppe, M., Arien, A., Bruining, M., Peeters, J., 2004. The use of polymer-based electrospun nanofibers containing amorphous drug dispersions for the delivery of poorly water-soluble pharmaceuticals. *Pharmazie* 59, 387–391.
- Driscoll, T.P., Nakasone, R.H., Szczesny, S.E., Elliott, D.M., Mauck, R.L., 2013. Biaxial mechanics and inter-lamellar shearing of stem-cell seeded electrospun angle-ply laminates for annulus fibrosus tissue engineering. *J. Orthop. Res.* 31, 864–870.
- Hu, X., Liu, S., Zhou, G., Huang, Y., Xie, Z., Jing, X., 2014. Electrospinning of polymeric nanofibers for drug delivery applications. *J. Control. Release* 185, 12–21.
- Huang, C., Lucas, B., Vervaeck, C., Braeckmans, K., Van Calenbergh, S., Karalic, I., Vandewoestyne, M., Deforce, D., Demeester, J., De Smedt, S.C., 2010. Unbreakable codes in electrospun fibers: digitally encoded polymers to stop medicine counterfeiting. *Adv. Mater.* 22, 2657–2662.
- Huang, C., Soenen, S.J., Rejman, J., Trekker, J., Chengxun, L., Lagae, L., Ceelen, W., Wilhelm, C., Demeester, J., De Smedt, S.C., 2012a. Magnetic electrospun fibers for cancer therapy. *Advan. Funct. Mater.* 22, 2479–2486.
- Huang, C., Soenen, S.J., Van Gulck, E., Vanham, G., Rejman, J., Van Calenbergh, S., Vervaeck, C., Coenye, T., Verstraelen, H., Temmerman, M., 2012b. Electrospun cellulose acetate phthalate fibers for semen induced anti-HIV vaginal drug delivery. *Biomaterials* 33, 962–969.
- Huang, C., Soenen, S.J., Gulck, E., Rejman, J., Vanham, G., Lacus, B., Geers, B., Braeckmans, K., Shahin, V., Spanoghe, P., 2014. Electrospun polystyrene fibers for HIV entrapment. *Polym. Advan. Technol.* 25, 827–834.
- Ignatious, F., Sun, L., Lee, C.P., Baldoni, J., 2010. Electrospun nanofibers in oral drug delivery. *Pharm. Res.* 27, 576–588.
- Keserü, G.M., Makara, G.M., 2009. The influence of lead discovery strategies on the properties of drug candidates. *Nat. Rev. Drug Discov.* 8, 203–212.
- Kostakova, E., Meszaros, L., Gregor, J., 2009. Composite nanofibers produced by modified needleless electrospinning. *Mater. Lett.* 63, 2419–2422.
- Kostakova, E., Seps, M., Pokorny, P., Lukas, D., 2014. Study of polycaprolactone wet electrospinning process. *Express Polym. Lett.* 8, 554–564.
- Li, J., Gao, F., Liu, L., Zhang, Z., 2013a. Needleless electro-spun nanofibers used for filtration of small particles. *Express Polym. Lett.* 7, 683–689.
- Li, X., Kanjwal, M.A., Lin, L., Chronakis, I.S., 2013b. Electrospun polyvinyl-alcohol nanofibers as oral fast-dissolving delivery systems of caffeine and riboflavin. *Colloids Surf. B* 103, 182–188.
- Lipinski, C.A., 2000. Drug-like properties and the causes of poor solubility and poor permeability. *J. Pharmacol. Toxicol.* 44, 235–249.
- Lipinski, C.A., Lombardo, F., Dominy, B.W., Feeney, P.J., 1997. Experimental and computational approaches to estimate solubility and permeability in drug discovery and development settings. *Adv. Drug Deliv. Rev.* 23, 3–25.
- Lukas, D., Sarkar, A., Pokorny, P., 2008. Self-organization of jets in electrospinning from free liquid surface: a generalized approach. *J. Appl. Phys.* 103, 084309.
- Lukas, D., Sarkar, A., Martinova, L., Vodsedalkova, K., Lubasova, D., Chaloupek, J., Pokorny, P., Mikes, P., Chvojka, J., Komarek, M., 2009. Physical principles of electrospinning (electrospinning as a nano-scale technology of the twenty-first century). *Text. Prog.* 41, 59–140.
- Macri, L.K., Sheihet, L., Singer, A.J., Kohn, J., Clark, R.A., 2012. Ultrafast and fast bioerodible electrospun fiber mats for topical delivery of a hydrophilic peptide. *J. Control. Release* 161, 813–820.
- Molnár, K., Nagy, Z.K., Mészáros, L., Marosi, G., 2012. Electrostatic spinneret and modified process for high-throughput production of nanofibers. *P1200677*.
- Molnár, K., Kostakova, E., Mészáros, L., 2014. The effect of needleless electrospun nanofibrous interleaves on mechanical properties of carbon fabrics/epoxy laminates. *Express Polym. Lett.* 8, 62–72.
- Nagy, Z.K., Nyúl, K., Wagner, I., Molnár, K., Marosi, G., 2010. Electrospun water soluble polymer mat for ultrafast release of Donepezil HCl. *Express Polym. Lett.* 4, 763–772.
- Nagy, Z.K., Balogh, A., Vajna, B., Farkas, A., Patyi, G., Kramarics, Á., Marosi, G., 2012. Comparison of electrospun and extruded soluplus-based solid dosage forms of improved dissolution. *J. Pharm. Sci.* 101, 322–332.
- Nagy, Z.K., Balogh, A., Drávavölgyi, G., Ferguson, J., Pataki, H., Vajna, B., Marosi, G., 2013. Solvent-free melt electrospinning for preparation of fast dissolving drug delivery system and comparison with solvent-based electrospun and melt extruded systems. *J. Pharm. Sci.* 102, 508–517.
- Nagy, Z.K., Wagner, I., Suhajda, Á., Tobak, T., Haraszts, A., Vigh, T., Sóti, P., Pataki, H., Molnár, K., Marosi, G., 2014. Nanofibrous solid dosage form of living bacteria prepared by electrospinning. *Express Polym. Lett.* 8, 352–361.
- Niu, H., Lin, T., 2012. Fiber generators in needleless electrospinning. *J. Nanomater.* doi:http://dx.doi.org/10.1155/2012/725950.
- Pelipenko, J., Kocbek, P., Govedarica, B., Rošic, R., Baumgartner, S., Kristl, J., 2013. The topography of electrospun nanofibers and its impact on the growth and mobility of keratinocytes. *Eur. J. Pharm. Biopharm.* 84, 401–411.
- Pouton, C.W., 2006. Formulation of poorly water-soluble drugs for oral administration: physicochemical and physiological issues and the lipid formulation classification system. *Eur. J. Pharm. Sci.* 29, 278–287.
- Prentis, R., Lis, Y., Walker, S., 1988. Pharmaceutical innovation by the seven UK-owned pharmaceutical companies (1964–1985). *Brit. J. Clin. Pharmacol.* 25, 387–396.
- Rosic, R., Kocbek, P., Pelipenko, J., Kristl, J., Baumgartner, S., 2013. Nanofibers and their biomedical use. *Acta Pharm.* 63, 295–304.
- Sebe, I., Szabo, B., Nagy, Z.K., Szabo, D., Zsidai, L., Kocsis, B., Zelko, R., 2013. Polymer structure and antimicrobial activity of polyvinylpyrrolidone-based iodine nanofibers prepared with high-speed rotary spinning technique. *Int. J. Pharm.* 458, 99–103.
- Six, K., Verreck, G., Peeters, J., Binnemans, K., Berghmans, H., Augustijns, P., Kinget, R., Van den Mooter, G., 2001. Investigation of thermal properties of glassy itraconazole: identification of a monotropic mesophase. *Thermochim. Acta* 376, 175–181.
- Sóti, P.L., Telkes, L., Rapi, Z., Tóth, A., Vigh, T., Nagy, Z.K., Bakó, P., Marosi, G., 2014. Synthesis of an aza chiral crown ether grafted to nanofibrous silica support and application in asymmetric Michael addition. *J. Inorg. Organomet. Polym.* 24, 713–721.
- Vardakou, M., Mercuri, A., Barker, S.A., Craig, D.Q., Faulks, R.M., Wickham, M.S., 2011. Achieving antral grinding forces in biorelevant in vitro models: comparing the USP dissolution apparatus II and the dynamic gastric model with human in vivo data. *AAPS PharmSciTech* 12, 620–626.
- Verreck, G., Chun, I., Peeters, J., Rosenblatt, J., Brewster, M.E., 2003. Preparation and characterization of nanofibers containing amorphous drug dispersions generated by electrostatic spinning. *Pharm. Res.* 20, 810–817.
- Vrbata, P., Berka, P., Stránská, D., Doležal, P., Musilová, M., Čižinská, L., 2013. Electrospun drug loaded membranes for sublingual administration of sumatriptan and naproxen. *Int. J. Pharm.* 457, 168–176.

- Wagner, I., Pataki, H., Balogh, A., Nagy, Z.K., Harasztos, A., Suhajda, Á., Marosi, G., 2011. Electrospun nanofibers for topical drug delivery. *Eur. J. Pharm. Sci.* 44, 148–149.
- Williams, G.R., Chatterton, N.P., Nazir, T., Yu, D.G., Zhu, L.M., Branford-White, C.J., 2012. Electrospun nanofibers in drug delivery: recent developments and perspectives. *Ther. Deliv.* 3, 515–533.
- Yan, J., Wu, Y.H., Yu, D.G., Williams, G.R., Huang, S.M., Tao, W., Sun, J.Y., 2014. Electrospun acid–base pair solid dispersions of quercetin. *RSC Adv.* 4, 58265–58271.
- Yu, D.G., Chian, W., Wang, X., Li, X.Y., Li, Y., Liao, Y.Z., 2013a. Linear drug release membrane prepared by a modified coaxial electrospinning process. *J. Membrane Sci.* 428, 150–156.
- Yu, D.G., Hu, M.H., Zhou, W., Chen, B.Y., Wang, X., 2013b. Electrospun ketoprofen sustained release nanofibers prepared using coaxial electrospinning. *Appl. Mech. Mater.* 395, 138–143.
- Yu, D.G., Liu, F., Cui, L., Liu, Z.P., Wang, X., Annie Bligh, S.W., 2013c. Coaxial electrospinning using a concentric Teflon spinneret to prepare biphasic-release nanofibers of helicid. *RSC Adv.* 3, 17775–17783.